

Topotactic Formation of Highly Conductive Organic Crystals —TTF-TCNQ—

T. MAEDA, H. KURATA, S. ISODA and T. KOBAYASHI*

Received August 22, 1989

Formation process of TTF-TCNQ complex in solid state has been investigated by electron microscopy and electron energy loss spectroscopy (EELS).

The complex crystals have been observed to grow topotactic on TCNQ single crystals by exposing the TCNQ to a vapor of TTF. The crystallographic correlation between original TCNQ and the complex has been observed by electron microscopy and the topotactic complex formation was found. The reaction process has been followed also by EELS and the process was analyzed quantitatively. It is confirmed that the electron microscopy connected with EELS is a powerful method for a quantitative study of the reaction process of a solid material.

KEY WORDS: TTF-TCNQ/ EELS/ Formation mechanism/ Organic thin film/

INTRODUCTION

It is desirable for a practical use or a fundamental study in research field that a highly conductive organic crystal can be obtained in a form of a well oriented thin film because the anisotropic nature of the organic material is most remarkably exhibited in this state. From this point of view, the present authors have investigated and reported the structure of TTF-TCNQ (Fig. 1) films obtained epitaxially by direct sublimation of TTF-TCNQ complex in vacuum¹⁾. In the epitaxial films many stacking faults have been found and deviation of the stoichiometric ratio of TTF to TCNQ from unity has been found. Such a non-stoichiometry might result from the difference in vapor pressures of TTF and TCNQ. Another method to make a well oriented thin film of a charge transfer complex was tried and described here.

EXPERIMENTAL

TCNQ epitaxial film was firstly made on (001) surface of KCl according to the same method reported in reference 2. The KCl crystal thus covered with the TCNQ film was cut into several pieces of 5×5 mm in sizes and sealed with a small amount of TTF powder in a glass Petri-dish. The dish was kept at a constant temperature in an air-bath whose temperature was controlled electrically.

Each piece of the KCl was taken out of the dish at an appropriate time interval. In order to be examined by electron microscopy, the TCNQ film or its reacted product was

* 前田尚志, 倉田博基, 磯田正二, 小林隆史: Laboratory of Crystal and Powder Chemistry, Institute for Chemical Research, Kyoto University, Uji, Kyoto 611.

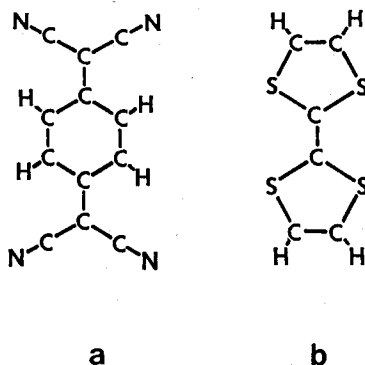


Fig. 1. Molecular structures of
 (a) tetracyanoquinodimethane (TCNQ) and
 (b) tetrathiafluvalene (TTF).

fixed on a copper grid or on a microgrid after dissolving the substrate KCl on pure water. An electron microscope equipped with an energy analyzer underneath the camera chamber was used which was operated at 100 kV. The detail of the system has been reported in reference 3.

RESULTS

Total aspect of TCNQ grown epitaxially on KCl is shown in Fig. 2(a) with its high resolution electron diffraction pattern and a selected area diffraction pattern. TCNQ crystallites in the film take multiple orientations relative to the substrate KCl. Every crystallite has the same crystal habit exhibiting its ac-plane as the film plane. A selected area electron diffraction pattern from one crystallite shown in Fig. 2(c) was obtained from the crystal encircled in Fig. 2(a). The diffraction pattern shows that the c-axis of the TCNQ coincides with the long axis of the crystallite. Eight sets of this pattern are superimposed, where the c^* -axis of each crystallite aligns parallel to or deviates $\pm 4^\circ$ and $\pm 18^\circ$ from the directions of KCl [100] or [010] as shown in Fig. 2(b). This means the epitaxially grown TCNQ takes multiple orientations in the film.

When these films were exposed to a vapor of TTF, they began to react forming fine needle crystallites on each TCNQ crystallite. At very early stage of the reaction, some fine needles can be observed on the TCNQ crystals. The electron micrograph shown in Fig. 3(a) exhibits a film at such stage. The selected area electron diffraction pattern from the encircled area in the micrograph is shown in Fig. 3(b) which exhibits still nearly the same aspect with Fig. 2(c), that is the main diffraction spots come from unreacted TCNQ crystals. In addition to the main spots, faint diffuse streaks and spots are also observable. They can be assigned to the fine needle crystals appeared newly.

In further reaction, the electron micrograph shown in Fig. 4 demonstrates more clearly the morphological change in the film caused by the reaction. A selected area electron diffraction pattern of this film shows that original TCNQ partly reacted with TTF resulting in a TTF-TCNQ complex and other part remains unreacted as shown in Fig. 4(b). On the equator of the diffraction pattern two series of the diffraction spots appear

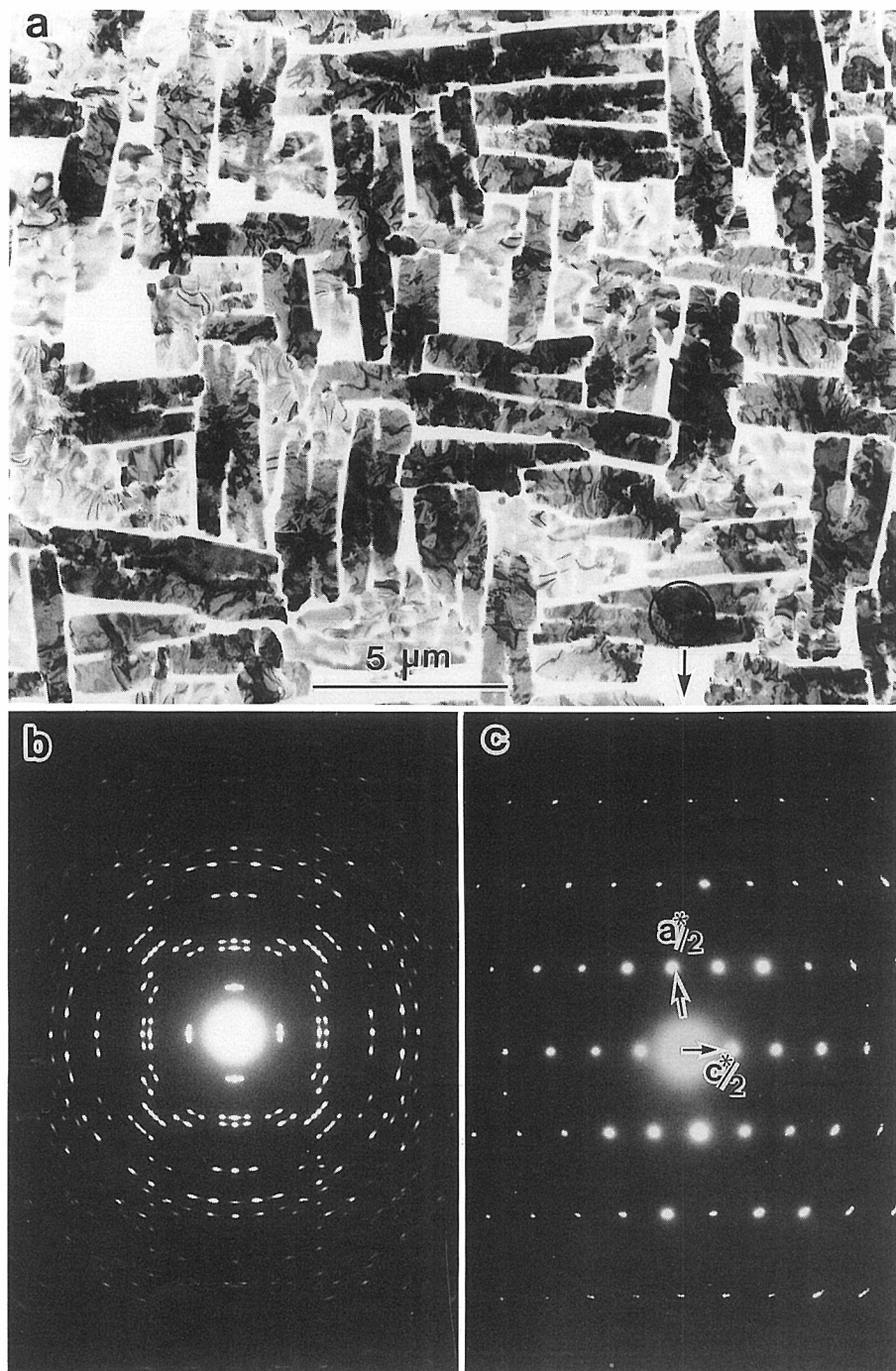


Fig. 2. Epitaxial film of TCNQ grown on KCl at 50°C (a) and high resolution electron diffraction pattern (b) from (a). A selected area electron diffraction pattern (c) was obtained from an encircled area in (a).

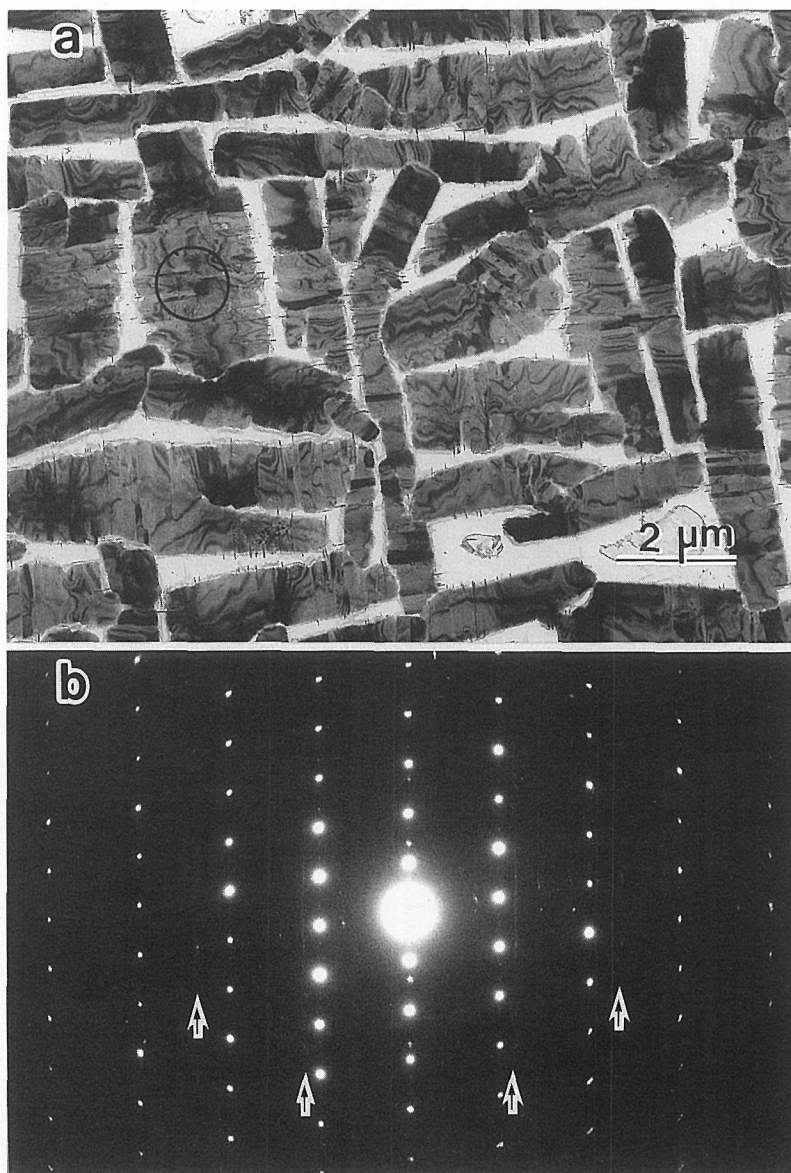


Fig. 3. Epitaxial film of TCNQ exposed to a vapor of TTF for one hour (a) and encircled area gives the diffraction pattern (b).

together. One is with the interval of $1/8.10 \text{ \AA}^{-1}$ and the other is with that of $1/11.9 \text{ \AA}^{-1}$. The layer lines can also be divided into two sets. One is composed of spots which are arranged in the same interval with those observed on the equator and marked with white arrows. This set is the same as that in Fig. 2(c) and shows the existence of unreacted TCNQ. The other set is composed of diffuse lines running parallel to the equator. The interval among the layer lines of this set is $1/3.77 \text{ \AA}^{-1}$. These extra layer lines and the extra spots on the equator marked with the black arrows are considered to be due to

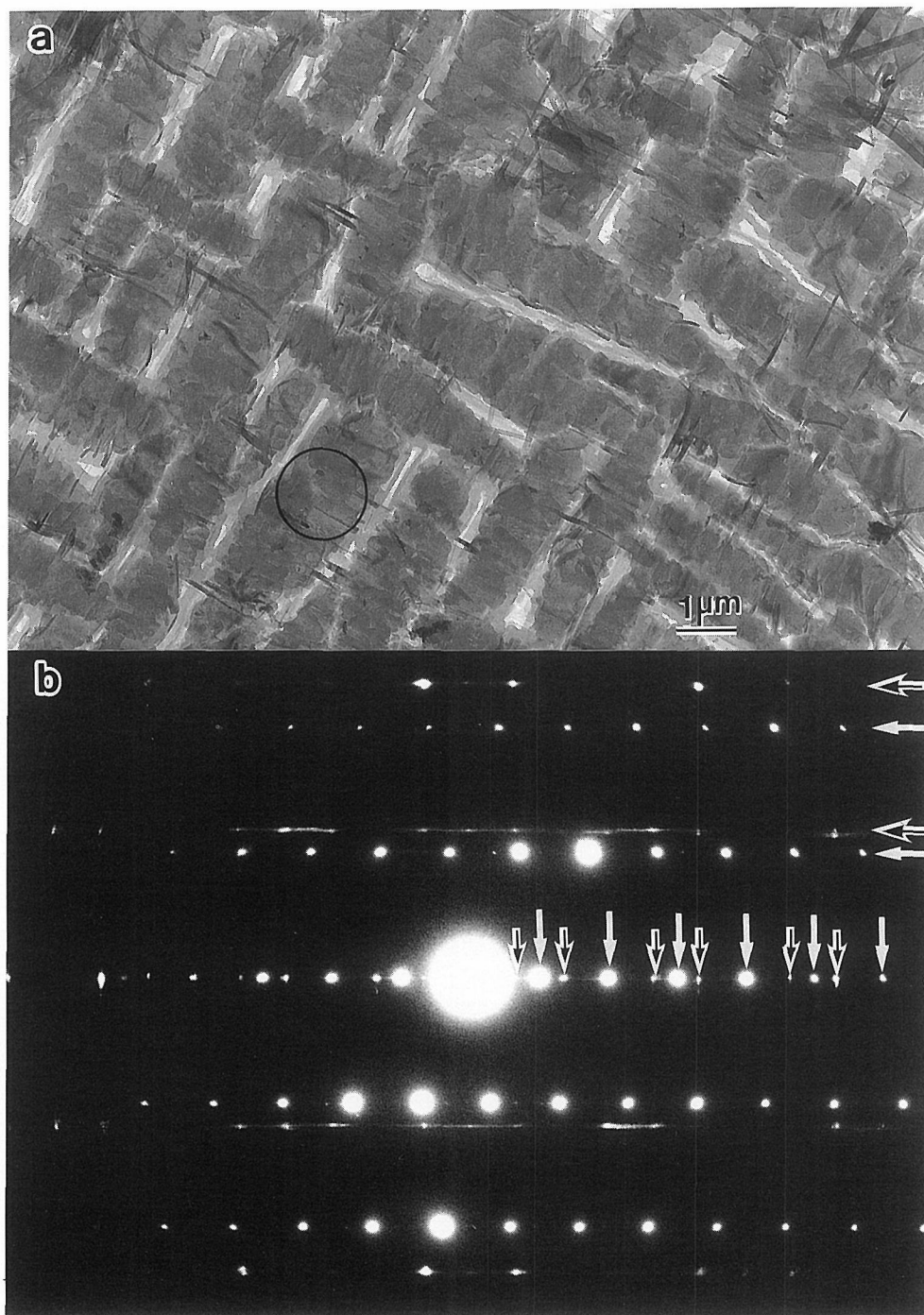


Fig. 4. An electron micrograph of TCNQ reacted partly with TTF (a) and its selected area electron diffraction pattern(b).

TTF-TCNQ complex on the basis of their periods which coincide well with the crystallographic data of the complex reported by Kistenmacher, Philips and Cowan⁴). The b-axis of the complex coincides with the needle axis and with the a-axis of the TCNQ mother crystal.

In addition to the appearance of fine needle crystallites, lattice defects were also produced in the TCNQ crystal itself. The defect lines are running parallel to the longer axis of the newly appeared needle crystallites. Furthermore the electron micrograph shows strong diffraction contrast which are observed on every TCNQ crystallite of the original and of those at the early stage of the reaction. They appear as black parts in the micrographs, but the contrast disappears and only grayish contrast remains at an advanced stage of the reaction. Each original TCNQ crystal is divided into many pieces along the a-axis, that is, shorter axis of the crystals. These facts suggest that the TCNQ mother crystals are largely distorted by the chemical reaction and the distortion is relaxed by introducing the defect along the a-axis of TCNQ.

The elemental ratio of the number of sulfur atoms to that of carbon, which also gives the molar ratio of TTF to TCNQ in the specimen partly reacted, was measured by means of electron energy loss spectroscopy. The elemental ratio was obtained by using the following formula⁵).

$$\frac{N_c}{N_s} = \frac{\sigma_s(\alpha, \Delta) \cdot I_c(\alpha, \Delta)}{\sigma_c(\alpha, \Delta) \cdot I_s(\alpha, \Delta)}$$

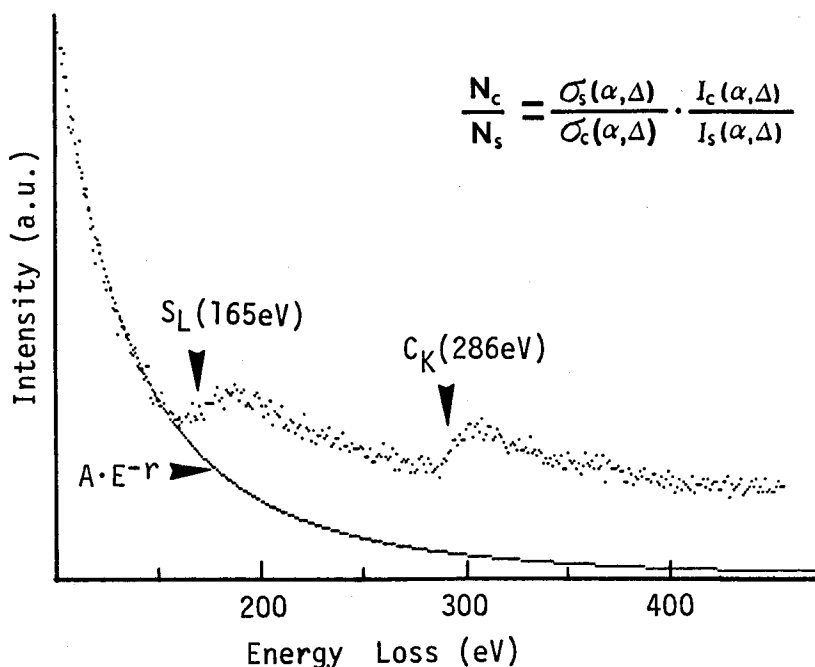


Fig. 5. Electron energy loss spectrum from TTF-TCNQ 1 : 1 complex. The base line was approximated as AE^{-r} .

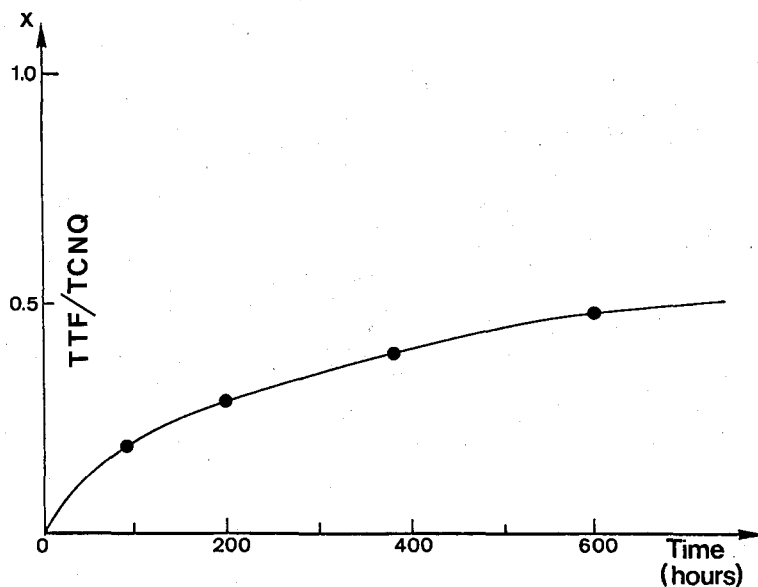


Fig. 6. The molar ratio of TTF to TCNQ in reaction intermediates are plotted against the reaction times.

Here, $I_s(\alpha, \Delta)$ and $I_c(\alpha, \Delta)$ are the integrated intensity of a respective core loss spectrum over an energy range Δ , α is the accepted scattering angle of inelastically scattered electrons and constant during the measurement (10 mrad.). σ_s and σ_c represent the partial scattering cross sections of electrons of sulfur L-shells and carbon K-shell.

The ratio σ_c/σ_s can be obtained from the observed intensity ratio for a compound of a known composition, that is, TTF-TCNQ thin crystal film prepared by epitaxial method³⁾, or from the theoretical calculations. The experimentally obtained ratio of σ_c/σ_s for TTF-TCNQ 1:1 complex prepared by vacuum deposition of the complex is equal to 0.11 for the energy window (Δ) of 100 eV. In Fig. 5 an EELS spectra of TTF-TCNQ 1:1 complex is demonstrated. The theoretically expected ratio is, however, 0.127 for the elemental ratio of TTF-TCNQ 1:1 complex, that is $N_s/N_c=4/18$. The calculation is performed by using the programs SIGMAK⁶⁾ and SIGMAL⁷⁾ developed by Egerton based on a hydrogen model. This difference in σ_c/σ_s might be due to non-stoichiometry in TTF-TCNQ 1:1 complex prepared from the vapor of the complex. Therefore, by adopting the theoretical value for σ_c/σ_s , we can estimate the elemental ratio N_c/N_s for the film produced by present solid reaction at some stages of the reaction process and calculated the molar ratio of TTF to TCNQ as shown in Fig. 6 where the ratios are plotted against the reaction times at 25°C.

DISCUSSIONS

The crystal of TCNQ belongs to a monoclinic space group of C2/c and has the following lattice constants⁸⁾, $a=8.906 \text{ \AA}$, $b=7.060 \text{ \AA}$, $c=16.395 \text{ \AA}$, $\beta=98.54^\circ$ and

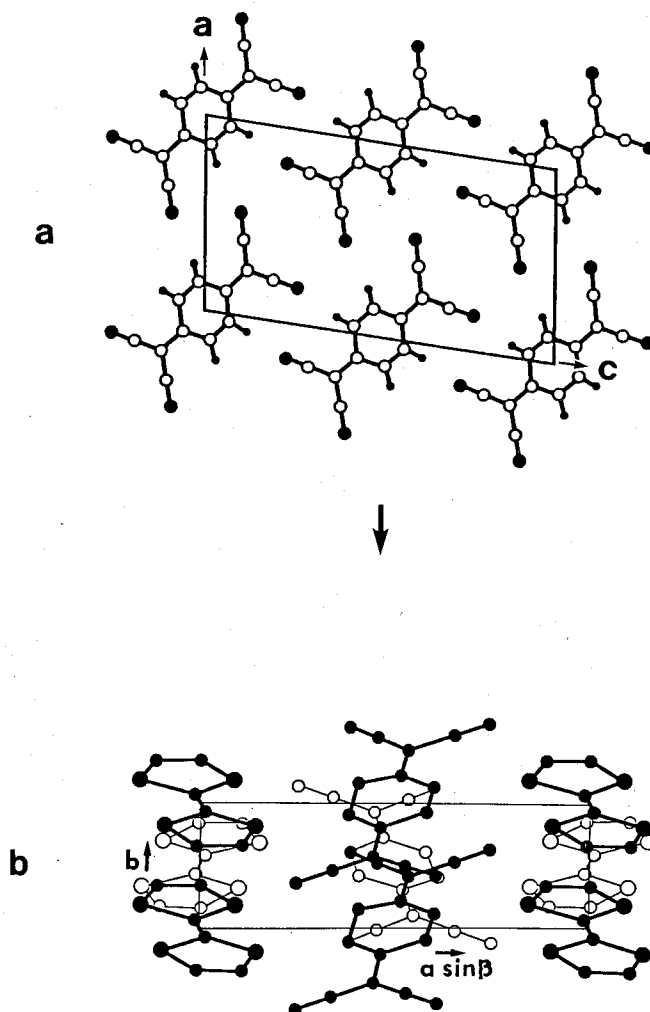


Fig. 7. Molecular arrangement of TCNQ projected on the ac -plane (a) and those of TTF-TCNQ seen along the c -axis (b). Here the axial relation obtained from Fig. 4 (b) is maintained between (a) and (b).

$Z=4$. According to the X-ray data, molecular arrangement of TCNQ projected onto the ac -plane is shown in Fig. 7(a). The molecules located at $(0.5, 0.5, 0.0)$ and $(0.5, 0.5, 0.5)$ in the unit cell are omitted in the figure. Each crystal forming the epitaxial film elongates along the c -axis as is evident from the selected area electron diffraction pattern shown in Fig. 2(c). For the reaction intermediate shown in Fig. 4(b) the electron diffraction pattern demonstrates that the formation of TTF-TCNQ occurs in topotactic. The diffraction spots with the reciprocal lattice units of $1/3.77 \text{ \AA}^{-1}$ and $1/11.9 \text{ \AA}^{-1}$ are assigned to TTF-TCNQ because they coincide well with the values of the (010) and (100) lattice spacings of TTF-TCNQ crystal grown from a solution, which belongs to a monoclinic space group of $P2_1/c$ and has the lattice constants of $a=12.298 \text{ \AA}$, $b=3.819 \text{ \AA}$, $c=18.468 \text{ \AA}$, $\beta=104.46^\circ$ and $Z=2^4$. Therefore the follow-

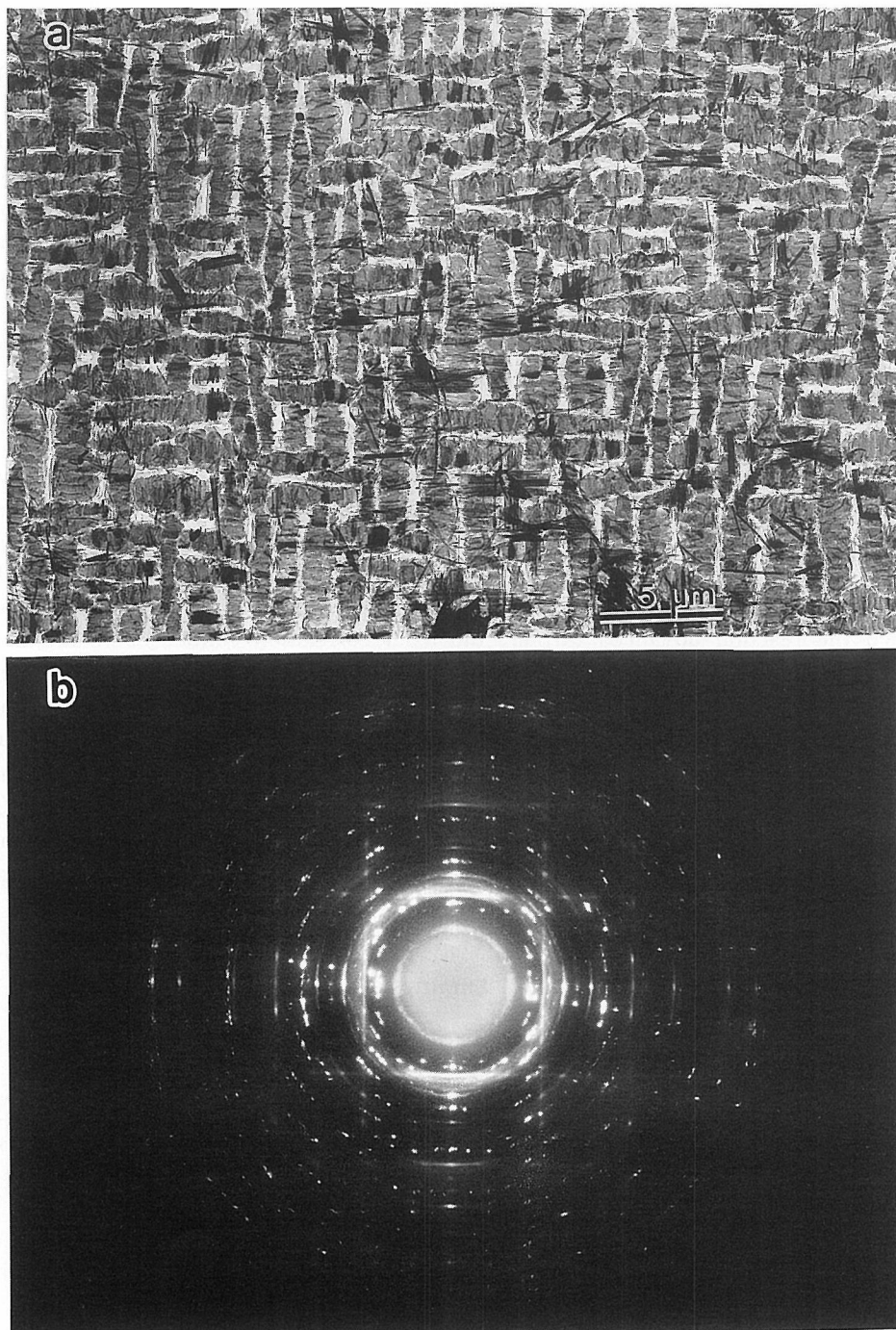


Fig. 8. Epitaxial film of TCNQ reacted with TTF for 600 hours at 25°C (a) and its high resolution electron diffraction pattern (b).

ing axial correlation between the TCNQ substrate and the reaction product TTF-TCNQ can be derived from the diffraction pattern shown in Fig. 4(b). That is, the b-axis and the a*-axis of the complex are parallel to the a-axis and the c*-axis of TCNQ, respectively. From these axial correlation, the change of molecular arrangement before and after the reaction of the complex formation can be deduced as shown in Fig. 7. It becomes evident that every TCNQ molecules rotate their long molecular axis about 45° around the molecular center in the plane including the axis and rise half out of the original plane. The distances between the centers of the TCNQ molecules in the original crystal are 8.906 Å/2 and 8.197 Å along the a- and c-axes, while those in the final reaction product are 3.819 Å and 12.298 Å along the b- and a-axes in their projections. Thus in order to form the complex the movement of TCNQ molecules is considered to be fairly large. On the other hand the reaction velocity to form the complex at 25°C is very slow especially at the advanced state of the reaction. As can be seen in Fig. 6, 50% of the original TCNQ still remains unreacted even after 600 hours.

The reaction seems to occur mainly on the surface of the TCNQ crystallites and also occurs outside the substrate TCNQ crystal, being suggested from newly formed needle-like crystals on the TCNQ. Therefore it is concluded that the formation of TTF-TCNQ complex does occur not only by diffusion of TTF molecules into TCNQ crystal, but also by direct vapor-vapor reaction near or on the original TCNQ crystal surfaces. When the reaction advanced further, the axial correlation cannot be maintained any more as one can see in Fig. 8 where the diffraction pattern from the complex almost becomes Debye-Scherrer rings. The topotactic or epitaxial relation between the substrate and the produced complex might be smeared during further complex formation and substrate-independent complex formation would proceed in such stage. The electron micrograph displays many needle-like crystallites which are TTF-TCNQ crystals fairly thickened. In order to discuss the reaction mechanism in more detail, the reaction rates at various temperatures should be measured so that the activation energy of the reaction can be obtained.

REFERENCES

- 1) K. Yase, O. Okumura, T. Kobayashi and N. Uyeda, *Bull. Inst. Chem. Res., Kyoto Univ.*, **62**, 242 (1984).
- 2) N. Uyeda, Y. Murata, T. Kobayashi and E. Suito, *J. Cryst. Growth*, **26**, 267 (1974).
- 3) K. Ishizuka, H. Kurata, T. Kobayashi and N. Uyeda, *J. Electron Microsc.*, **35**, 343 (1986).
- 4) T. J. Kistenmacher, T. E. Philips and D. O. Cowan, *Acta Cryst.*, **B30**, 763 (1974).
- 5) R. F. Egerton, *Electron Energy Loss Spectroscopy in the Electron Microscope*, Plenum Press, New York and London, 1986.
- 6) R. F. Egerton, *Ultramicros.*, **4**, 169 (1979).
- 7) R. F. Egerton, 39th Ann. Proc. Electron Microsc. Soc. Am., **1981**, 198 (1981).
- 8) R. E. Long, R. A. Sparks and K. N. Trueblood, *Acta Cryst.*, **18**, 932 (1965).